Development of a vibration isolator with dry friction damping

Rene Boonen, Paul Sas

KULeuven, Faculty of Engineering Sciences, Mechanical Engineering, PMA

Celestijnenlaan 300B, 3001 Leuven, Belgium, Email: rene.boonen@kuleuven.be

Introduction

Vibration isolation is a key issue in technical engineering, ranging from buildings to machines until precision and micro-mechanics. Just a few examples from an quasi unlimited number of applications are air conditioning equipment in buildings, engines and wheel suspension in transport, sensitive optical equipment, hard drives and so on.

The linear vibration isolator consists of the classical mass-spring-damper configuration [1, 2, 3, 4] where the undesired vibration has to pass from the environment through the spring-damper component to the suspended object or vice versa.

The transfer function magnitude of the force transmission through the suspension component is presented in figure 1 for three different types of suspensions. The vibration isolation occurs at frequencies above the zero-dB crossing of the transfer function amplitude. The difference between the transfer function amplitude and the 0-dB is a measure for the isolation performance.

- *undamped spring*: The isolation characteristic (magenta line in figure 1) is a -40 dB/decade decline above the eigenfrequency f_n. At the eigenfrequency, the transfer function magnitude tends to infinity. Disturbances occurring at the eigenfrequency will lead to unacceptable amplitudes. This kind of suspension is used for rotating machinery, such as turbines, or for acoustic measurement rooms, where the suspension resonance will not be excited.

- *spring-damper element*: The isolation characteristic (red line in figure 1) tends to a -20 dB/decade decline above the eigenfrequency f_n, which is less performant than the undamped spring. This is caused by the viscous damper in parallel with the spring were through the force will be transmitted in the high frequency range. The transition frequency where the isolation characteristic alters from -40 dB/decade to -20 dB/decade is $f_t = \frac{1}{2\,\pi}\,\frac{k}{c}$, wherein k is the spring constant and c the damper constant. At eigenfrenquency, the transfer function magnitude is limited by the damper. These suspension components are used in applications where excitation at eigenfrequency can occur, such as wheel suspensions in vehicles.

- *hysteresis damping*: Hysteresis damping or internal material damping is dominantly present in elastomeric materials. The damping is expressed as a complex spring constant in the frequency domain. The isolation characteristic (blue line in figure 1) remains a -40 dB/decade decline above the eigenfrequency f_n. At eigenfrequency, the transfer function magnitude is limited by the imaginary part of the complex spring constant. Rubber suspension elements are widely used in engineering. The disadvantages are mainly of technological nature: the elastic modulus is highly temperature dependent and the material exhibits considerable creep.

The use of non-linear suspension components is also widely exploited [3, 4, 5], such as non-linear spring and damping characteristics, the use of mechanisms to introduce non-linear displacement relations and the use of different types of dampers, such as dry friction. For example, a dry friction damper in parallel with a spring and a viscous damper has been analyzed [5]. The suspension component is very effective to damp the vibrations. However, at small amplitudes, the dry friction damper blocks and the vibrations are transmitted to the suspended object without any attenuation.

In this research, a new type of suspension component using dry friction has been developed which is able to combine the -40 dB/decade isolation characteristic, considerable damping at resonance and robust against environmental influences such as temperature, in the six degrees of freedom.

First, the principle of the suspension component will be discussed. Then, the functioning of the component will be analyzed using an unidirectional model and Hamilton's method is applied to deal with the non-linear effects. The model parameters such as the spring constants and the friction will be identified. Then, the model will be evaluated using a shock excitation and the resulting response will be discussed. Finally, the model will be evaluated from data measured on an experimental setup.

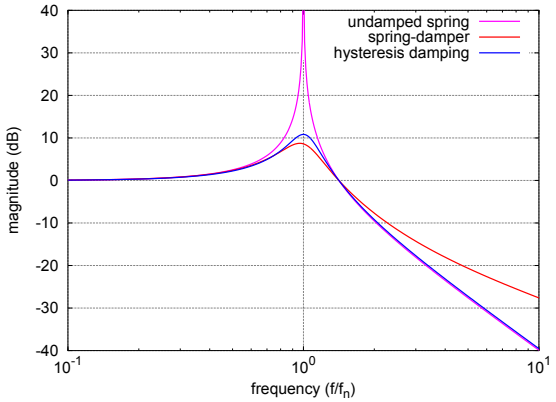

Figure 1: Force transmission characteristic of different vibration isolator principles.

Principle of the dry friction suspension component

The principle of the suspension component is presented in figure 2. It consist of a spring wire bended in a 3-D Ω-

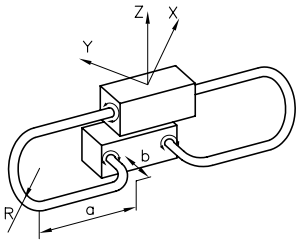

Figure 2: Principle of the dry friction suspension component.

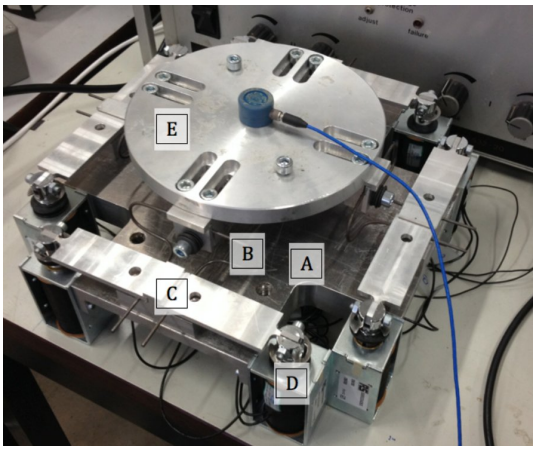

Figure 3: Photograph of the experimental setup with four dry friction suspension components.

shape. The shape of the wired spring allows some design freedom to diversify the resonance frequencies in the X-, Y- and Z-direction. The wire is embedded in the connection blocks. Due to the displacement of the connection blocks as a consequence of a shock or vibration, reaction torques appear at the connection interfaces. When the vibration amplitudes remain small, the spring wire remains fixed in the connection blocks and the isolator behaves as an undamped spring. When these torques overcome the internal dry friction, the connection slips in the interface and vibration energy is dissipated by the suspension component.

Figure 3 shows a photograph of the experimental setup. Four suspension components are located between the base plate A and the suspended object E. The object has a mass of 0.97 kg. The Ω-shaped spring wire B is fitted at the suspended object such it can rotate with dry friction. The dimensions of the spring wire are $R = 12$ mm, $a = 20$ mm and $b = 16$ mm. At the base plate side at position C, the friction of the wire ends can be altered by electro-magnetic coil actuators D. These actuators will allow to optimize the damping for different disturbing forces using a semi-active control strategy. By positioning the four suspension components under 90°, the damping mechanism is active in all six degrees of freedom.

Analysis of the suspension component

To demonstrate the proof of concept, the analysis is carried out in the height direction as a SDOF system. The

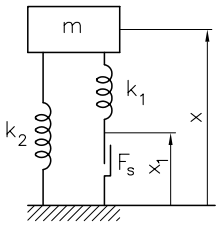

Figure 4: One-dimensional model of the dry friction suspension component.

model, presented in figure 4, consists of the suspended mass m, the spring k_1 connected in series with the dry friction damper with a slipping force F_s which form the damper branch and the spring k_2 connected in parallel with the damper branch. As the suspension component exhibits non-linear behavior, the method of Hamilton [6] is used to set up the equations of motion. The method uses a scalar potential function, called the Hamiltonian, which is the sum of the kinetic and potential energy of the suspended system, expressed in displacement, momentum and time as independent variables. Taking the derivatives of the Hamiltonian to displacement and momentum results in the set of first order equations of motion, which can be solved numerically by any ODE-solver.

The kinetic energy E_k and potential energy E_{p2} of the spring k_2 are:

$$E_k = \tfrac{1}{2}\, m\, \dot{x}^2 \quad \text{and} \quad E_{p2} = \tfrac{1}{2}\, k_2\, x^2 \tag{1}$$

The potential energy E_{p1} of the spring k_1 and the dissipated power P_s in the dry friction damper are dependent of the position x_1 which in turn is dependent of the position x of the mass m. In the case that the mass position is larger than $\frac{F_s}{k_1}$, the damper is in motion while the spring length of k_1 is constant.

So, the potential energy E_{p1} of the spring k_1 and the dissipated power P_s in the dry friction damper are:

$$E_{p1} = \frac{1}{2}\, k_1\, (\frac{F_s}{k_1})^2 \quad \text{and} \quad P_s = F_s\, \text{sign}(\dot{x})\, \dot{x} \tag{2}$$

wherein the sign-function is -1 if $\dot{x} < 0$, 0 if $\dot{x} = 0$ and $+1$ if $\dot{x} > 0$.

When the mass displacement becomes sufficiently close to the equilibrium position such that the force in the damper branch becomes smaller than F_s, the damper blocks and the spring k_1 moves. In this case, the potential energy E_{p1} of the spring k_1 and the dissipated power P_s in the dry friction damper are:

$$E_{p1} = \frac{1}{2}\, k_1\, (x - \frac{F_s}{k_1})^2 \quad \text{and} \quad P_s = 0 \tag{3}$$

Once the displacement is through the equilibrium position and becomes larger than $-\frac{F_s}{k_1}$ at the negative side, the damper is activated again and the spring k_1 will be

again constant in length. So, the potential energy E_{p1} of the spring k_1 and the dissipated power P_s in the dry friction damper are:

$$E_{p1} = \frac{1}{2} k_1 \left(-\frac{F_s}{k_1}\right)^2 \quad \text{and} \quad P_s = F_s \,\text{sign}(\dot{x})\, \dot{x} \tag{4}$$

The transitions between deactivating the damper and activation again takes place at the two positions $x = \frac{F_s}{k_1}$ at the positive side and $x = -\frac{F_s}{k_1}$ at the negative side. This will be expressed by the two switching functions:

$$\delta_1 = \delta(x - \tfrac{F_s}{k_1}) \quad \text{and} \quad \delta_2 = \delta(x + \tfrac{F_s}{k_1}) \tag{5}$$

The function $\delta(y)$ is 0 if $y < 0$ and +1 if $y \geq 0$.

Combining the expressions (1)-(5) results in the expressions for the kinetic energy, potential energy and dissipated power:

$$\begin{aligned} E_k &= \frac{1}{2} m\, \dot{x}^2 \\ E_p &= \frac{1}{2} k_2\, x^2 + \frac{1}{2} k_1 \left[x\,(1-\Delta) - \frac{F_s}{k_1}\right]^2 \\ P_s &= F_s \,\text{sign}(\dot{x})\, \dot{x}\, \Delta \end{aligned} \tag{6}$$

which are valid for each position x of the suspended mass. The switching function $\Delta = \delta_1 + \delta_2$.

Once the expressions (6) for the kinetic energy, potential energy and dissipated power are known, the equations of motion using Hamilton's method can be set up. The momentum p_x will be:

$$p_x = \frac{\partial E_k}{\partial \dot{x}} = m\, \dot{x} \tag{7}$$

The Hamiltonian which is the sum of the kinetic and potential energy, expressed in momentum, displacement and time will be:

$$H = \frac{1}{2} \frac{p_x^2}{m} + \frac{1}{2} k_2\, x^2 + \frac{1}{2} k_1 \left[x\,(1-\Delta) - \frac{F_s}{k_1}\right]^2 \tag{8}$$

The force expression will be:

$$\begin{aligned} \dot{p}_x &= F_l - \frac{\partial P_s}{\partial \dot{x}} - \frac{\partial H}{\partial x} \\ &= F_l - F_s \,\text{sign}(p_x)\, \Delta \\ &\quad - k_2\, x - k_1 \left[x\,(1-\Delta) - \frac{F_s}{k_1}\right](1-\Delta) \end{aligned} \tag{9}$$

with F_l an external applied force.

Ultimately, the result is a set of two first order differential equations of motion:

$$\begin{cases} \dot{x} = \dfrac{p_x}{m} \\ \dot{p}_x = F_l - F_s \,\text{sign}(p_x)\, \Delta \\ \qquad\quad -k_2\, x - k_1 \left[x\,(1-\Delta) - \dfrac{F_s}{k_1}\right](1-\Delta) \end{cases} \tag{10}$$

which can be solved by any ODE-solver.

Determination of the spring constants

The spring constants k_1 and k_2 will be determined from a FEM-analysis of the suspension construction as presented in figure 2. The analysis will be carried out for two cases, one with the wire ends free rotating in the mounting blocks, the other one with the wire ends fixed.

The first case corresponds to the spring k_2 because the spring k_1 does not change its length during the motion. The second case corresponds to the sum of the spring $k_1 + k_2$, as the damper is now blocked and the two springs are simply in parallel. The resulting deformations of the wire are presented in figure 5. From these deformations, $k_2 =$

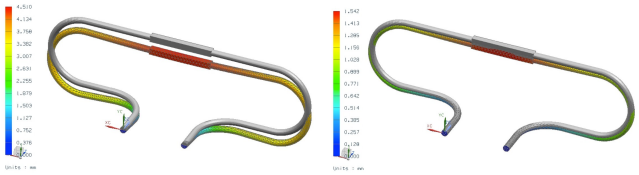

Figure 5: FEM-Analysis of the spring wire of a suspension component. *Left:* wire ends free; *Right:* wire ends fixed.

26.6 kN/m and $k_1 = 52.2$ kN/m. The friction force $F_s =$ 14N is determined from experiments. Using these data in the equations of motion (10) with an initial displacement $x_0 = 0$ and an initial velocity of $v_0 = 1.7$ m/s results in the impulse response presented in figure 6. The most

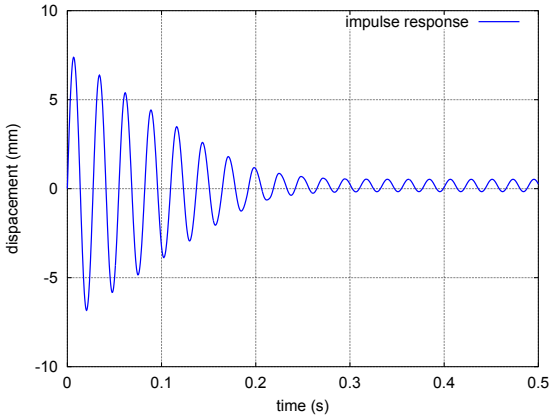

Figure 6: Simulated displacement of the suspended mass excited by an impulse.

interesting phenomena observed in the plot are:

1. In the first 0.2 s of the response, the damper is engaged. The decrease of the displacement magnitude each half period amounts $\frac{F_s}{k_1}$. The frequency can be approximated by $f = \frac{1}{2\,\pi} \sqrt{\frac{k_2}{m}}$. The damping mechanism is very efficient.

2. After a transition at 0.2 s, the remaining motion is an undamped vibration with a maximum amplitude of $\frac{F_s}{k_1}$. The frequency is increased compared to the first part of the motion and is determined by $f = \frac{1}{2\,\pi} \sqrt{\frac{k_1+k_2}{m}}$.

3. The equilibrium of the undamped vibration does not occur at $x = 0$. The dry friction damper blocks

somewhere between $-\frac{F_s}{k_1}$ and $\frac{F_s}{k_1}$, depending on the initial conditions. In practice, the exact position of the equilibrium will not be predictable. The total magnitude, i.e. the equilibrium position with thereupon superposed the vibration amplitude will never exceed the interval $[-\frac{F_s}{k_1}, \frac{F_s}{k_1}]$.

Experimental evaluation

The experimental setup, presented in figure 3, has been realized. The measurements have been carried out using an impulse hammer and an accelerometer in the center of the suspended mass. First, the acceleration response of the mass is recorded in time domain and plotted in figure 7 in red line, together with the second derivative of the displacement signal presented in figure 6 in blue line. The spring constants k_1 and k_2 have been derived from the FEM-analysis, the friction force has been estimated from the experiment and used in the simulation. The friction force can be adapted on the experimental setup using the electro-magnetic actuators in a range between 5 N and 54 N.

The measured response exhibits the same behavior as the predicted one. The acceleration amplitude decreases quasi linearly until the amplitude becomes to small to engage the friction damper. Then, the vibration amplitude remains constant. In the experimental setup of course, this amplitude will become zero after some seconds. The eigenfrequency of the setup in the undamped situation is quasi equal to the simulated one. The difference in frequency between simulation and experiment with active friction damper is due to the assumption that the spring ends are free which is not fully correct. Nevertheless, this assumption is sufficient in the design stage of the suspension component.

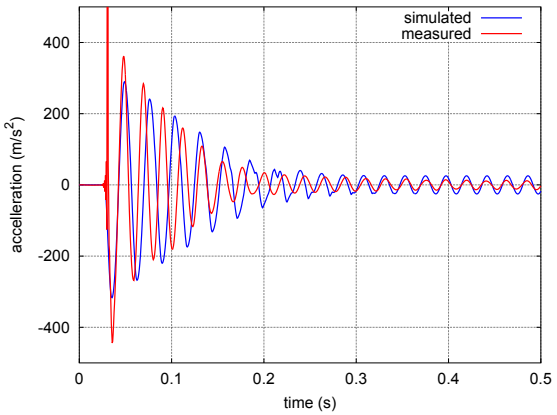

Figure 7: Comparison of the simulated with the measured acceleration of the suspended mass excited by an impulse.

The measured frequency spectrum, presented in figure 8 (left) in red line, has been averaged over 10 hammer hits. The simulated spectrum in blue line has been calculated from the simulated acceleration signal presented in figure 7. The resonance amplitude is limited to about 10dB, while the slope of the isolation part of the spectrum remains −40 dB/decade. Also, a measurement of the acceleration of the suspended mass has been carried out

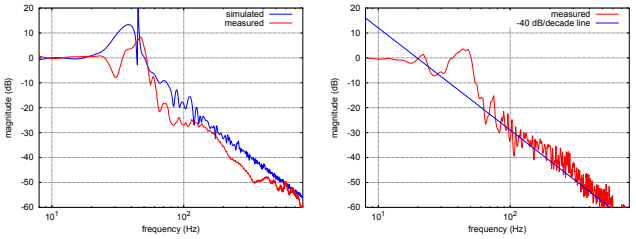

Figure 8: *left*: Spectra of the simulated and the measured displacements corresponding to the time signals presented in figure 7. *right*: Spectrum of the acceleration measured through the suspension compared with a −40 dB/decade line.

whereby the base plate is excited by hammer hits. The spectrum, averaged over 10 hammer hits, is presented in figure 8(right) and is compared to a −40 dB/decade line. It demonstrates that the isolation characteristic is equivalent to the undamped spring.

Conclusion

A new type of suspension component has been developed. It consist of an Ω-shaped spring wire which ends can slip in their mountings. By positioning these components under 90° around the suspended object, the suspension functions in all six degrees of freedom. A model of the suspension component has been set up and analyzed using Hamilton's equations of motion to deal with the non-linear phenomena. It is based on a series connection of a spring with a coulomb damper, which in turn is connected in parallel with a second spring. An experimental setup has been realized whereupon the suspension components are validated using hammer impulses. The observed response is an efficiently damped sinusoidal motion which turns into an undamped sinusoid with small amplitude. In the spectrum, the resonance has been limited in magnitude to 10 dB and the isolation characteristic remains −40 dB/decade equivalent to the undamped spring.

References

[1] J.P. Den Hartog: Mechanical vibrations, McGraw-Hill, New York, (1956).

[2] G. Genta: Vibration dynamics and control, Springer, New York, (2008).

[3] R. Ibrahim: Recent advances in nonlinear passive vibration isolators, Journal of Sound and Vibration, Vol. 314, (2008), pp. 371-452.

[4] C. Ho, Z. Lang, S. A. Billings: Design of vibration isolators by exploiting the beneficial effects of stiffness and damping non-linearities, Journal of Sound and Vibration, Vol. 333, (2014), pp. 2489-2505.

[5] M. S. Hundal: Response of a base excited system with coulomb and viscous friction, Journal of Sound and Vibration, Vol. 64, No. 3, (1979), pp. 371-378.

[6] C. Lanczos, The variational principles of mechanics, Dover publications, New York, (1986).